JOURNAL OF GUIDANCE, CONTROL, AND DYNAMICS
Vol. 23, No. 3, May–June 2000

Accommodating a Class of Actuator Failures in Flight Control Systems

R. A. Hess,* W. Siwakosit,† and J. Chung‡
University of California, Davis, Davis, California 95616

A technique for the design of flight control systems that can accommodate a set of actuator failures is presented. As employed herein, an actuator failure is defined as a change in the parametric model of the actuator that can adversely affect actuator performance. The technique is based on the formulation of a fixed feedback topology that ensures at least stability in the presence of the failures in the set. The fixed compensation is obtained from a loop-shaping design procedure similar to quantitative feedback theory and provides stability robustness in the presence of uncertainty in the vehicle dynamics caused by the failures. System adaptation to improve performance after actuator failure(s) occurs through a static gain adjustment in the compensator followed by modification of the system prefilter. Precise identification of the vehicle dynamics is unnecessary. Application to a single-input/single-output design using a simplified model of the longitudinal dynamics of the NASA High-Angle-of-Attack Research Vehicle is discussed. Non-real-time simulations of the system, including a model of the pilot, demonstrate the effectiveness and limitations of the approach.

Introduction

THE requirements that will accompany the design of future, high-performance aircraft, whether inhabited or uninhabited, will likely include some ability to automatically reconfigure the aircraft flight control system to accommodate control effector failure(s) and/or damage to the airframe itself. The advent of uninhabited combat air vehicles[1–4] will certainly increase research activity in this area, as will recent emphasis on airline safety.[5] Thus, the design of reconfigurable or restructurable flight control systems is of continuing importance to the research community. Reconfigurable control systems are those possessing the ability to accommodate system failures automatically through on-line self-modification. Reconfigurable control is a challenging design problem, as it usually entails failure detection, system identification, and on-line controller redesign. A sampling of this research can be found in Refs. 6–15.

The design philosophy to be discussed herein will be applied to the problem of failure of one or more of the actuators that drive the thrust/aerodynamic effectors in a flight control system, for example, elevator and thrust-vectoring nozzles. Attention will be focused on maintaining stability and performance in the presence of these failures. The flight control scenario to be examined assumes that the human pilot is controlling the vehicle when failure occurs and will resume control after reconfiguration is completed. Although actuator failures constitute only a subset of possible damage that can occur to a flight vehicle, the ability to accommodate such damage in a flight control system is pertinent for the following reason: The control effectors that the actuators drive are powerful force and moment producers. Thus, if a design methodology can provide stability and performance robustness in the presence of failure of these devices, there is reasonable hope that it can serve as a candidate reconfigurable design methodology for other classes of problems, for example, airframe damage.

Conceptually, the design approach to be discussed is considerably less complex (and admittedly less mathematically sophisticated) than others that have been proposed (e.g., Refs. 6–15) in that much of the flight control system remains unchanged in the presence of the actuator failure. This design philosophy was pursued for simplicity and for its reliance on proven frequency-domain design techniques. It may be hyperbole to refer to the adaptive formulation employed here as a reconfigurable control system; however, for the sake of brevity, this will be done.

Received 19 February 1999; revision received 21 September 1999; accepted for publication 24 September 1999.

*Professor and Vice Chairman, Department of Mechanical and Aeronautical Engineering, One Shields Avenue. Associate Fellow AIAA.

†Graduate Student, Department of Mechanical and Aeronautical Engineering.

‡Postdoctoral Researcher, Department of Mechanical and Aeronautical Engineering.

Approach

Design Preliminary Considerations

The research to be described will first concentrate on ensuring that the aircraft stability and command augmentation system (SCAS) is as robust as possible to the effects of actuator failure(s). This implies requiring at least stability in the presence of the failures to be considered and will depend on the existence of redundant aerodynamic/propulsive control effectors, that is, effectors that provide control authority comparable to that of the effector(s) whose actuator(s) has failed. Although the existence of redundant effectors may seem to be a significant requirement, the reconfiguration technique being discussed is intended to accommodate complete as well as partial failure of actuators. An important part of the design procedure for the undamaged aircraft is the inclusion of software rate limiters, whose purpose is to improve system performance when actuator saturation occurs. The design and utility of such software rate limiters have been discussed in the literature.[16]

Design Philosophy

The philosophy behind the design approach rests on the established tenet that careful application of frequency-domain loop-shaping techniques can provide a SCAS (with fixed compensator) that exhibits stability and performance robustness in the presence of significant uncertainty in the dynamics of the vehicle being controlled. An attempt to extend this approach to encompass uncertainty brought about by actuator failures would likely produce compensators with unacceptably high bandwidth. However, reducing the requirements on the compensator to providing stability and performance robustness for the undamaged vehicle and only stability robustness for the damaged vehicle can offer a significant reduction in required system bandwidth. Creating an adaptive system with a modest amount of reconfiguration capability would allow some of the performance robustness, lost in the failures, to be regained. Thus, the approach to be discussed will distribute the responsibility for accommodating actuator failures between a fixed compensation element or elements and a relatively simple adaptive system.

Design Framework

Figure 1 is a diagrammatic representation of the design framework to be pursued. Note that full-envelope design is the goal. One begins with a set of healthy aircraft models (i.e., those with undamaged

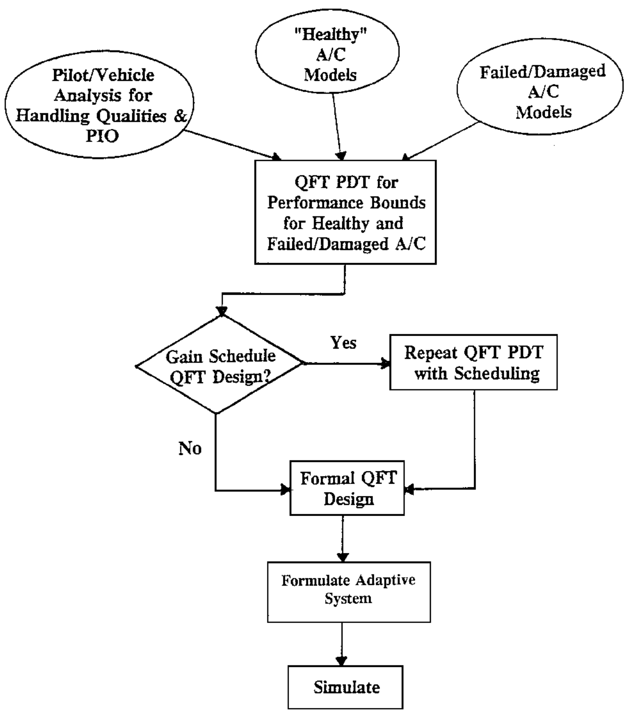

Fig. 1 Framework for reconfigurable flight control system design.

actuators) at the flight conditions representative of the vehicle's operational envelope. To this set is appended the failed aircraft models, that is, those with damaged actuators. Performance goals for the healthy aircraft are established that ensure satisfactory handling qualities with no tendencies for pilot-induced oscillations. Analytical means addressing these latter design constraints are available.[17] Failure detection will not be addressed in what follows. It will be assumed that the failure of an actuator(s) will be detected, either by health monitoring of the devices themselves or through anomalies in the vehicle response to command inputs. The nature of the failures and the particular actuator(s) involved will not be assumed to be known. Finally, the design and simulation utilize a simple perturbation model of the aircraft. This simplification was felt to be warranted in this study because a SCAS, albeit one with damaged actuators, will always be in operation, thus mitigating the effects of trim changes that could occur with actuator damage.

Predesign Technique

A quantitative feedback theory (QFT) predesign technique (PDT)[18] is employed and flight control laws (compensation elements) are created with the PDT that attempt to 1) meet the performance goals for the undamaged aircraft, 2) ensure stability for the damaged aircraft, and 3) minimize the necessity of dynamic reconfiguration, that is, that requiring changes in the dynamic compensation elements of the SCAS. The possibility of gain scheduling with flight condition is included with the aim of reducing controller bandwidths. Finally, and if necessary, a formal QFT design can be undertaken in which the approximate control laws obtained with the PDT are evaluated and modified, if necessary.[18] Note that, as with any QFT design, stability can be guaranteed not just for those failures that are explicitly included in the failed set, but for any failures that exhibit dynamics with magnitude and phase characteristics that fall within the bounds defined by the members of the original failure set.

Adaptive Logic

Although the final QFT design will ensure satisfactory handling qualities and immunity to pilot-induced oscillation (PIO) for the healthy aircraft, only stability will be sought with the damaged aircraft. Hence, an adaptive system is created for the purpose of recovering as much performance as possible under conditions of actuator failure. Concentrating on a single-input/single-output (SISO) system [or a single loop of a multi-input/multi-output (MIMO) system] for the purposes of exposition, the adaptive logic consists of two parts. The first part is simply a static gain that multiplies the compensator obtained from the PDT approach (that emulates a QFT design). The multiplicative term is adjusted based on the system response to a test input. The ability of a single, variable gain to ensure stability of the pilot/vehicle systems is a result of the PDT approach. The second part of the logic involves a reconfiguration of the SCAS prefilter as a lead-lag element with parameters also dependent on the system response to the test input. This reconfiguration recoups SCAS bandwidth lost when stability is maintained through the static gain variation just described.

The adaptive logic is implemented as follows: After detection of a failure, a test square-wave input is applied to the SCAS (with pilot inputs eliminated). A simple classification technique is employed in which responses are first characterized as oscillatory (positive overshoot) and nonoscillatory (negative overshoot, that is, no overshoot and sluggish response). Based on this classification, the static gain term is varied until the responses meet a percent overshoot (PO) criterion, for example, $PO_{min} \le PO \le PO_{max}$. The time from the initiation of each pulse of the square wave to the response variable's achieving its maximum value is used to determine the form of the prefilter lead term. As just described, the reconfiguration formulation appears very ad hoc in nature. However, it is based on relatively simple, time- and frequency-domain relationships that can be examined in real time as part of the adaptive logic.

Simulation

Non-real-time and piloted simulation complete the design process outlined in Fig. 1. In the former simulation category, realistic models of pilot tracking behavior should be included.

Example

Design Overview

Predesign Technique

A brief example of a SISO system can be offered that demonstrates the design procedure. Figure 2 shows the former NASA High-Angle-of-Attack Research Vehicle (HARV). For the purposes of this example, attention is focused on longitudinal pitch control with redundant effectors consisting of the elevator (stabilator) and pitch-thrust vectoring. For brevity's sake, only a single flight condition is employed here. Thus, the performance bounds one finds in a typical QFT design are not employed. Figure 3 shows the pitch-rate flight control system diagram and pilot-loop closure for pitch-attitude tracking.

The predesign technique can be briefly summarized as follows. The compensator $G_c(s)$ is chosen as

$$G_c(s) = \omega_c/s \cdot 1 \Big/ \left[(q/u_c)|_{nom} \cdot (s/15\omega_c + 1)^p\right] \qquad (1)$$

where ω_c is the crossover frequency of the SCAS loop transmission q/q_e, $(q/u_c)|_{nom}$ is the q to u_c transfer function for the undamaged vehicle, and p is the excess of poles over zeros in $(q/u_c)|_{nom}$ with the transfer functions defined in Fig. 3.

The minimum crossover frequency is the found for which 1) the variation in $|(q/q_c)(j\omega)|$ is satisfactory for the undamaged vehicle

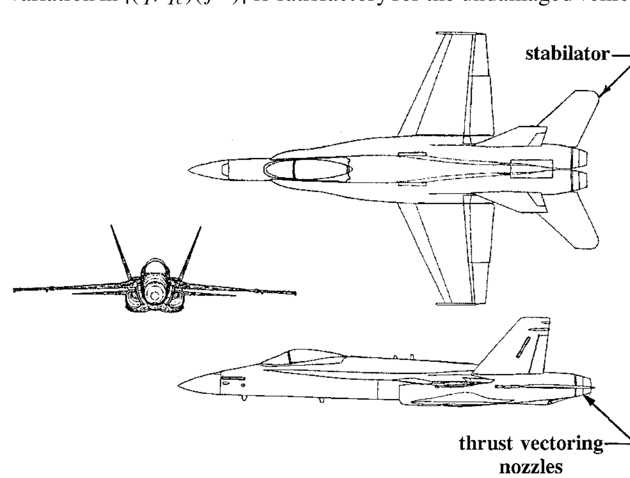

Fig. 2 NASA HARV.

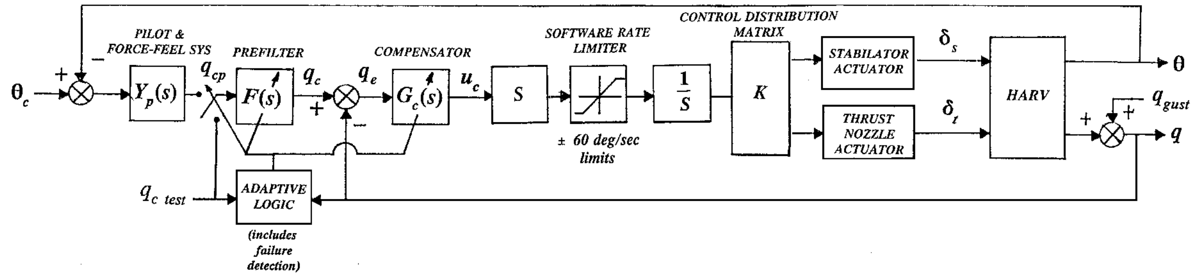

Fig. 3 Pitch-rate SCAS and pilot/vehicle system.

given uncertainty introduced by considering different flight conditions and/or by errors in the vehicle model; 2) rejection of constant disturbances injected at the actuator inputs is minimized, thus minimizing the effects of nonzero null failures of the actuators; and 3) q/q_c is stable for all actuator failures considered. Prefilter dynamics $F(s)$ are then selected to yield predicted level one handling qualities with no PIO susceptibility for the undamaged vehicle. Care must obviously be taken in employing Eq. (1) if $(q/u_c)|_{\text{nom}}$ is unstable or possesses right-half plane zeros (neither of which occurred in this example). In the former case, ω_c must be greater than the real part of the unstable pole with the most positive real part, and pole-zero cancellation with the plant must be avoided, whereas in the latter case, ω_c must be less than the real part of the nonminimum phase zero with the most positive real part, and again, pole-zero cancellation with the plant must be avoided.

Appendix A gives the vehicle and (healthy) actuator dynamics, taken from Ref. 19. In addition, characteristics of the cockpit force/feel system to be included in the pilot/vehicle simulation are given. Also note that rate and amplitude limiting were included in the actuator models. Appendix B lists the actuator failure characteristics. A set of 35 combinations of actuator failures define the damaged vehicle set. This set includes the undamaged or healthy aircraft. It must be emphasized at this juncture that, with the exception of zero values for the gains K_E and K_T (null failures of the actuators) the parametric variations indicated in Appendix B do not represent realistic models of specific actuator failure modes. Rather, they represent a convenient means of introducing significant magnitude and phase variations in the linear description of the actuator dynamics for the sake of exposition. Figure 4 shows the Bode diagrams of the transfer functions q/u_c from Fig. 3 with the 35 failures. Note the 20-dB variation in magnitude and the phase variation at 10 rad/s exceeding 270 deg. Compensation and prefilter elements $G_c(s)$ and $F(s)$ were obtained using the PDT of Ref. 18 ensuring that the criteria described earlier were satisfied. This meant predicted level one handling qualities and no predicted PIO tendencies with the undamaged aircraft and stability with the damaged aircraft, with the potential of crossover-frequency variation (through a multiplicative gain) stabilizing the SCAS. The handling and PIO predictions were accomplished using the pilot modeling procedure described in Ref. 20. The resulting $G_c(s)$, and $F(s)$, and ω_c were

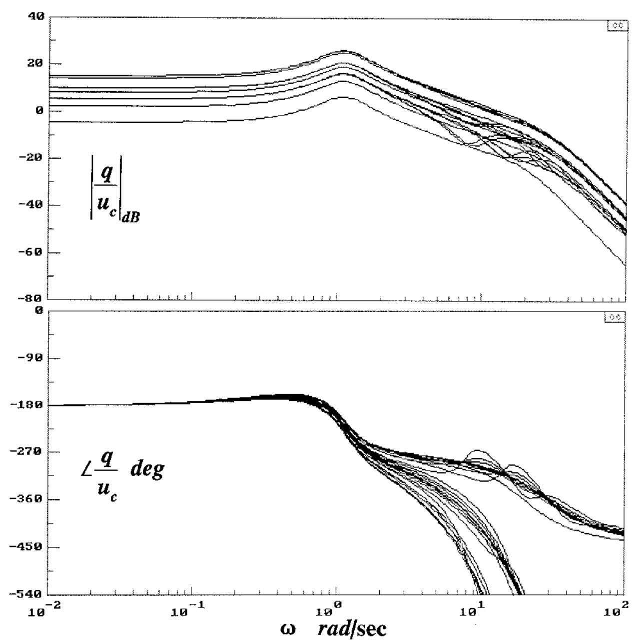

Fig. 4 Bode plots of transfer functions of vehicle plus actuators with actuator failures.

the presence of actuator saturation under normal operation,[16] and have thus been included as part of the SCAS design. For their implementation the software limiters require a control distribution matrix $\boldsymbol{K}$ that distributes the single pseudocontrol u_c to the two actuators, one commanding stabilator position and the second commanding pitch thrust nozzle position. For rate limiter implementation, each row of $\boldsymbol{K}$ contains only a single nonzero entry equal (or proportional) to the magnitude of the rate limit of the actuator that it affects. In the relatively simple example here, $\boldsymbol{K}$ is thus chosen as

$$\boldsymbol{K} = \begin{bmatrix} 1 \\ 1 \end{bmatrix} \tag{3}$$

$$G_c(s) = \frac{-20.2[s^2 + 2(0.35)1.12s + 1.12^2][s^2 + 2(0.6)20s + 20^2][s^2 + 2(0.69)30s + 30^2]}{s(s + 0.493)[s^2 + 2(0.606)21.14s + 21.14^2](s + 37.5)^3}, \qquad F(s) = \frac{0.3s + 1}{0.1s + 1}, \qquad \omega_c = 2.5 \text{ rad/s} \tag{2}$$

The complexity of $G_c(s)$ is due to the PDT that involves inversion of the plant dynamics (including actuators) as indicated in Eq. (1). Simplification of $G_c(s)$ is possible, but was not pursued herein. Figure 5 shows the Bode diagram of $G_c(s)$. Because $|G_c(j\omega)|$ does not increase beyond the 2.5 rad/s crossover frequency, a modest cost of feedback is involved.[18]

Software Rate Limiters and Control Distribution Matrix

The software rate limiters will be discussed only briefly herein. These devices have shown promise for improving performance in

The software limiters are implemented so that the maximum rate command to either actuator does not exceed its rate limit, here 60 deg/s for either actuator as indicated in Appendix A. Note that the differentiating s in Fig. 3 is always subsumed into the strictly proper $G_c(s)$.

Fixed Compensation

Figure 6 shows the SCAS loop transmissions (q/q_e in Fig. 3) for the 35 failures on a Nichols chart. Note that closed-loop stability is in evidence. For comparison, curve a in Fig. 7 is a similar diagram

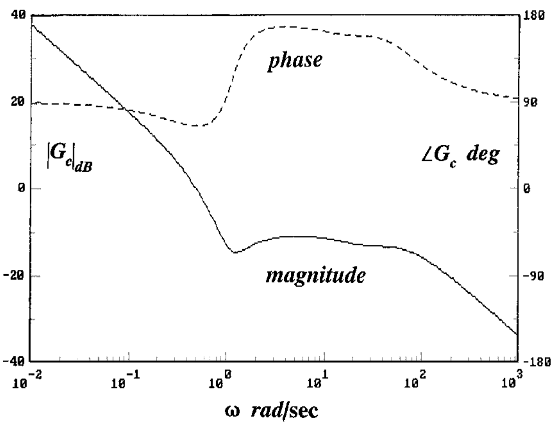

Fig. 5 Bode plot of PDT compensator $G_c(s)$.

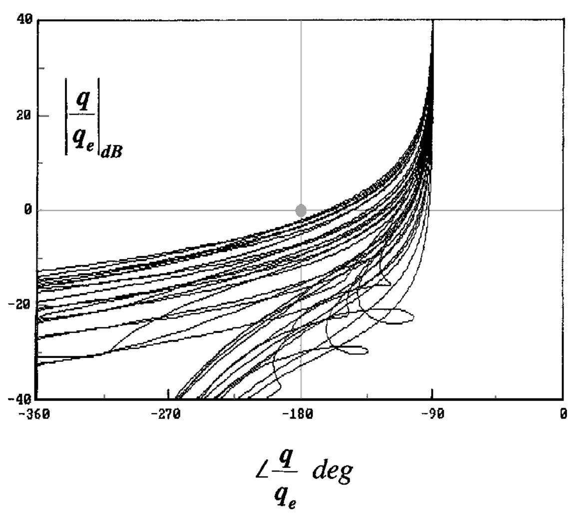

Fig. 6 Nichols chart plot of SCAS loop transmissions for damaged aircraft.

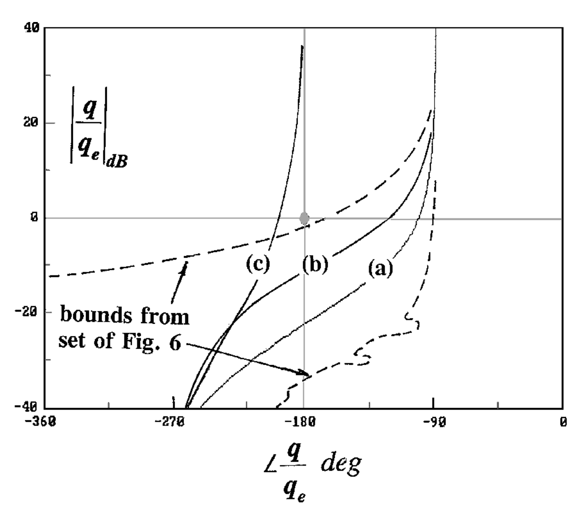

Fig. 7 Nichols chart plot of SCAS loop transmissions for a) undamaged aircraft, b) damage not in modeled set, and c) damage outside bounds of modeled set.

for the undamaged aircraft. Figure 8 demonstrates the extreme variation in closed-loop behavior of the SCAS that occurs with failed actuators. Here, the SCAS step responses (q–q_{cp} from Fig. 3) for all the failure cases are shown. By contrast, Fig. 9 shows the step response for the undamaged aircraft.

Adaptive Logic

As alluded to in the preceding section the adaptive logic that defined the reconfigurable system was predicated on real-time ex-

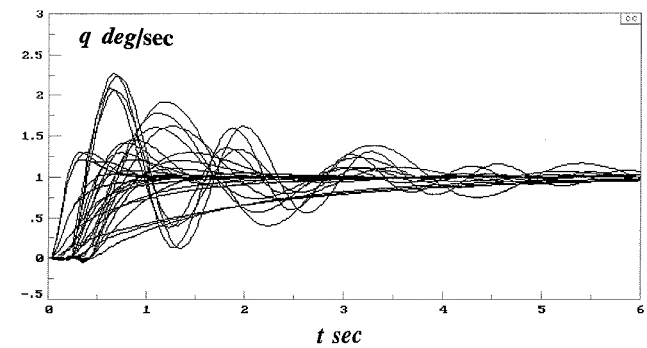

Fig. 8 SCAS step responses (q–q_{cp}) for damaged aircraft.

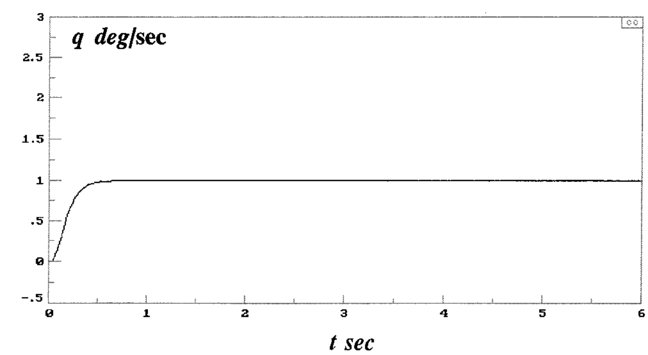

Fig. 9 SCAS step response (q–q_{cp}) for undamaged aircraft.

amination of the pitch-rate response $q(t)$ to a square-wave command injected as shown in Fig. 3, with pilot inputs excluded from the system. Based on the bandwidths of q/q_c for the failed systems with the fixed compensation of Eq. (2), the duration of each pulse of the square wave was selected as 4 s, with the first 2 s of the response to each pulse examined in the adaptive system. The static multiplying term included in $G_c(s)$ was $(1 + K_D)$ where K_D was initially zero. K_D was then varied in the following manner: If the response to the square-wave pulse indicated negative overshoot, then K_D was increased. If the response indicated an overshoot, K_D was decreased. A negative overshoot was defined as no overshoot and a value less than the commanded value 2 s from the initiation of the square-wave pulse. The adaptive logic was such that changes in K_D were inversely proportional to the amount of overshoot (positive or negative) as follows:

$$K_D(0) = \pm 0.1$$

$$K_{D_1}(kT) = K_D[(k-1)T] \pm \frac{1}{|0.05 \cdot \mathrm{PO}|}$$

$$K_d(kT) = \pm\min\left\{\left|K_{D_1}(kT)\right|, 1.2 \cdot |K_D[(k-1)T]|\right\} \tag{4}$$

with the + or − sign dependent on whether a positive or negative overshoot was in evidence. Equation (4) implies that after the initial 0.1 value, changes in K_D were relatively small early in the adaptive procedure. This was done for the following reason: It is possible that large turbulence disturbances could mask the nature of the q-step response of the vehicle. Thus, a K_D change of incorrect sign could occur early in the adaptation. If this incorrect change were large enough, the SCAS could be destabilized. The overshoot criterion that determined whether reconfiguration was to be initiated, and, if initiated, when it should be terminated was

$$-5\% \le \mathrm{PO} \le 10\% \tag{5}$$

Selection of $\mathrm{PO}_{\max}$ and $\mathrm{PO}_{\min}$ was based on the desire to allow K_D variation to provide most of the transient response improvement for the SCAS.

The prefilter reconfiguration was employed to improve the transient response characteristics of q/q_{cp} beyond that obtainable with variation in the SCAS compensator gain $(1 + K_D)$ alone. It involved

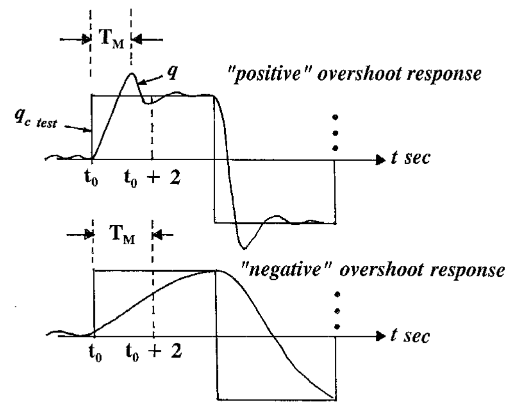

Fig. 10 Definition of q response effective time constant.

first removing the prefilter of Eq. (2) when a failure had been detected, that is, setting $F(s) = 1.0$. After the final K_D value had been obtained, a new prefilter was inserted in the system, given by

$$F'(s) = \frac{[(T_M/4)s + 1]^2}{(0.1s + 1)^2} \tag{6}$$

where T_M is the effective time constant of the q response. In Eq. (6), T_M was the time after reconfiguration when the response variable q achieved its maximum value within the duration of any pulse of the square-wave input (or 2.0 s, whichever was smaller). This T_M definition is shown in Fig. 10 positive and negative overshoot cases. Equation (6) was obtained by first approximating the bandwidth ω_B of q/q_c as

$$\omega_B \approx 4/T_M \tag{7}$$

Two simple zeros for the prefilter $F'(s)$ were then placed at $s = -\omega_B$. The $F'(s)$ given by Eq. (6) implies amplification of the pilot's command in the frequency range beyond $4/T_M$. This amplification is attributable to the severe nature of the failures in the modeled set, many of which introduced large, serial time delays in the SCAS. Thus, the characteristics of $F'(s)$ are a necessary part of the price to be paid for reconfiguration with the present scheme. Note that the impact of this amplification will be a function of q/q_c with failed actuators.

Simulation

Pilot Model

The efficacy of the design technique just outlined was investigated in a non-real-time simulation. A realistic pilot model was included[20] with dynamics based on the undamaged vehicle. A crossover frequency of 1.5 rad/s was selected as representing aggressive tracking behavior. The pilot model took the form

$$Y_p(s) = \frac{2.5 \cdot 10^5 \cdot e^{-0.2s}}{[s^2 + 2(0.146)14.1s + 14.1^2][s^2 + 2(0.778)28.9s + 28.9^2]} \tag{8}$$

After reconfiguration, the pilot model gain was adjusted so as to maintain the original 1.5 rad/s crossover frequency. This is equivalent to limiting pilot adaptation to the reconfigured dynamics (or damaged dynamics in the case where no reconfiguration is allowed) to a change in gain. In practice, it would be advisable to reduce the prefilter gain (say by 50%) as part of the reconfiguration so as to minimize the possibility of PIO tendencies. Gain reductions such as this have been linked to the elimination of PIOs in some pilot-in-the-loop simulations.[21]

Tracking Task

The pitch-attitude tracking task of Fig. 3 was simulated wherein the pilot closed a pitch-attitude loop, with q_{cp} serving as the pilot command to the SCAS. A pseudorandom sum of sinusoids provided the tracking command θ_c. The root-mean-square value of this command was 5.7 deg (0.1 rad). In addition, turbulence was included in the simulation by injecting a random pitch-rate disturbance with an rms value of 0.57 deg/s (0.01 rad/s) into the vehicle pitch-rate response. During reconfiguration, no pilot inputs were allowed. After reconfiguration, the pilot model resumed tracking the sum of sinusoids command as just described.

Simulation Examples

System performance was evaluated for each of the 35 failures. Space permits only a discussion of two of the most extreme cases. Figure 11 shows the pilot/vehicle tracking performance for the undamaged vehicle. Figure 12 shows the performance after reconfiguration for a failure in which the thrust nozzle actuator fails completely (in the null position) and the stabilator actuator suffers a 50% reduction in effectiveness or steady-state gain. Figure 13 shows the performance without reconfiguration. As mentioned earlier, when no reconfiguration was allowed, the pilot/vehicle crossover frequency was still adjusted to maintain the 1.5 rad/s crossover frequency after failure. This permitted a fair comparison with the tracking performance when reconfiguration was allowed. Figure 14 shows the reconfiguration responses to the failure of Fig. 12, and Fig. 15 shows the corresponding increments in, and final value for, K_D. Figure 16 shows the pilot/vehicle tracking performance following a failure in which the thrust nozzle actuator has again

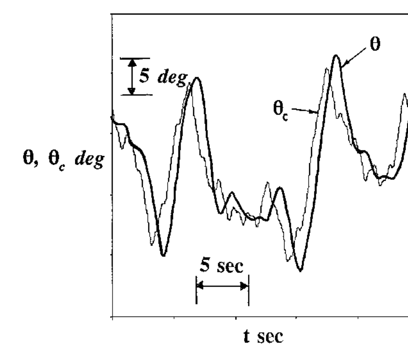

Fig. 11 Pilot/vehicle pitch-attitude tracking performance for undamaged aircraft.

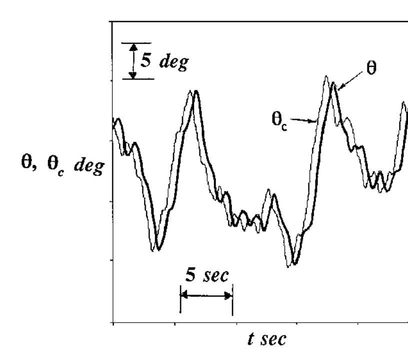

Fig. 12 Pilot/vehicle pitch-attitude tracking performance for damaged aircraft after reconfiguration: thrust actuator failed completely, stabilator with 50% effectiveness.

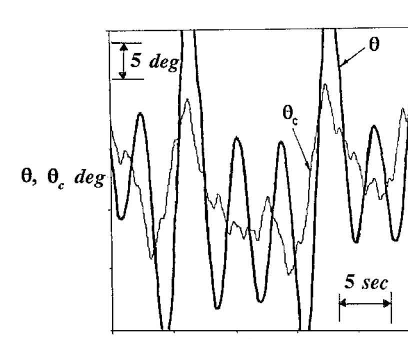

Fig. 13 Pilot/vehicle pitch-attitude tracking performance for aircraft damaged as in Fig. 12 but no reconfiguration.

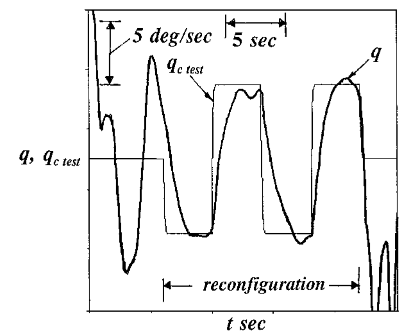

Fig. 14 Reconfiguration responses for aircraft damaged as in Fig. 12.

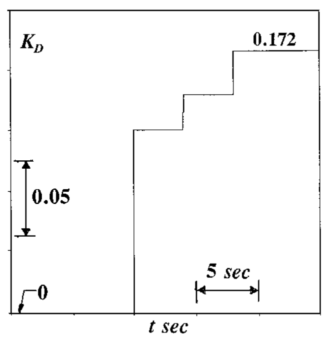

Fig. 15 K_D variation during reconfiguration of Fig. 12.

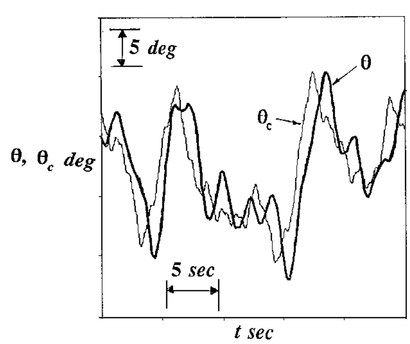

Fig. 16 Pilot/vehicle pitch-attitude tracking performance for damaged aircraft after reconfiguration: thrust actuator failed completely, stabilator with added 0.2-s delay.

failed completely and the stabilator actuator has a damaged-induced 0.2 s added time delay. In this case, when no reconfiguration was allowed, the pilot/vehicle system was unstable. Before reconfiguration for the two cases just presented, the q–q_c responses of the damaged vehicles were sluggish and highly oscillatory, respectively. In the reconfigurations for these two failures, T_M in Eq. (6) was 2.0 s. In the first of the reconfigurations, the elapsed time from beginning to end of reconfiguration until the final K_D value was obtained was 12 s, whereas for the second, the time was 36 s. The average reconfiguration time for all 35 configurations was 25.2 s, with the longest being 68 s. This average did not include those cases (11 in number) for which no reconfiguration was necessary, that is, the damaged vehicle was found to meet the overshoot requirements of inequality (5). Performance was always found to improve with the adaptive system when reconfiguration was found to be necessary.

Of interest is the simulation of a failure that was not a member of the modeled set. As mentioned earlier, the only constraint here is that the diagram of the loop transmission q/q_e of the unmodeled failure must lie within the bounds of the loop transmissions of all of the modeled cases on the Nichols chart. Curve b in Fig. 7 shows one such unmodeled failure that meets this criterion. In this failure the thrust nozzle actuator fails completely, the steady-state gain of the stabilator actuator increases by 50%, and the undamped natural frequency of the actuator is reduced from 30 to 10 rad/s. Figure 17 shows the tracking performance of the pilot/vehicle system with

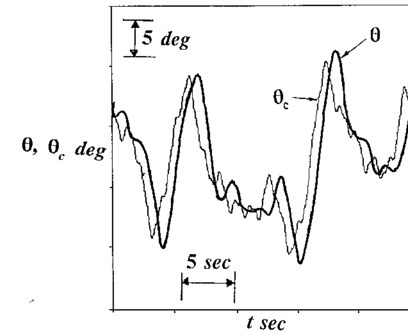

Fig. 17 Pilot/vehicle pitch-attitude tracking performance for damaged aircraft not in modeled set, no reconfiguration required.

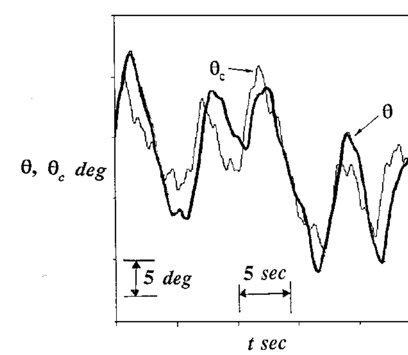

Fig. 18 Pilot/vehicle pitch-attitude tracking performance for damaged aircraft assuming actuator health monitoring.

this failure. In this instance, the criterion of inequality (4) was met without reconfiguration, and so the SCAS and prefilter dynamics remain unchanged. The tracking performance is seen to be quite satisfactory.

Also of interest is the simulation of a failure in which the resulting loop transmission is neither among the modeled set nor within the bounds of the modeled set in Fig. 6. One such failure was studied in Ref. 22 and represents a case in which the position feedback loop of the actuator was opened. With this failure the actuator dynamics are those of a velocity rather than a position servomechanism. Thus, an additional integration is introduced into the loop. This failure was implemented on the stabilator actuator here. The resulting loop transmission is shown as curve c in Fig. 7, where it is seen to violate the bounds from Fig. 6. As the Nichols chart indicates, the linear SCAS was unstable with this failure and reconfiguration was not possible. This example indicates one important limitation of the methodology, that is, failures falling outside the bounds of the modeled set may not be successfully reconfigured.

The failure just described could be accommodated within the current methodology with sufficiently fast actuator health monitoring. Actuators exhibiting significant input/output abnormalities (e.g., the 90-deg phase lag of the velocity servomechanism here) could be taken off-line. This removal would then correspond to one of the failure models ($K_E = 0$) and could be successfully reconfigured. To demonstrate this, the failure with the open position loop on the stabilator actuator was again simulated. Now, however, 2 s after the failure (simulating the detection time of a health monitoring system) the stabilator actuator was taken off-line with the stabilitor frozen at the angle achieved 2 s after the failure. The adaptive algorithm was then initiated. Convergence was achieved in 68 s with $K_D = 2.219$, and $T_D = 2.0$ s. Figure 18 shows the tracking performance after reconfiguration. Without reconfiguration for this failure but with the stabilator actuator taken off-line, the pilot/vehicle system was unstable.

Utility of Software Rate Limiters

Because the software rate limiters have been included in the design methodology, and because no significant rate limiting occurred in the 35 failure configurations simulated, a simulation involving artificially low actuator rate limits was conducted. These limits of 10 deg/s on each of the actuators were considered to be the characteristics of healthy, undamaged actuators. One of the failure modes considered earlier was again simulated in which the thrust actuator failed completely and the stabilator actuator provided 50% effectiveness. For the purpose of exposition, the pilot/vehicle response to a step pitch command rather than the sum of sinusoids was investigated after reconfiguration had occurred. Figure 19 shows the response of the undamaged system. Figure 20 shows the responses of the damaged system without and with reconfiguration. Note the improved performance with reconfiguration. Figure 21 shows the stabilator rate limiting occurring after reconfiguration. This is not rate limiting in the normal sense, however. The actuator is merely being driven by the software limiter up to its maximum rate, but no more.[16] For the reconfigured case, $K_D = 0.743$, $T_M = 2.0$ s, and the elapsed time from beginning to end of reconfiguration was 44 s. As in the earlier examples, the pilot gain was adjusted to yield a 1.5-rad/s crossover frequency after failures. The caveat here, however, is that this gain adjustment was made on the linear system, that is, where rate limiting was absent. Note that when the software rate limiters were removed in the reconfigurable design the pilot/vehicle system was unstable after reconfiguration. This emphasizes the importance of including the software limiters in the control architecture.

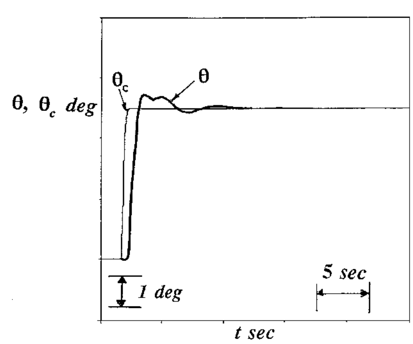

Fig. 19 Pilot/vehicle pitch-attitude tracking performance for undamaged aircraft, with actuator rate limiting of 10 deg/s.

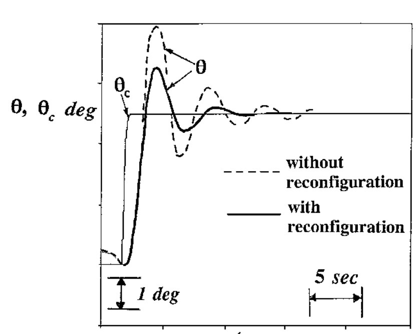

Fig. 20 Pilot/vehicle pitch-attitude tracking performance for aircraft damaged as in Fig. 12, with actuator rate limiting of 10 deg/s, without and with reconfiguration.

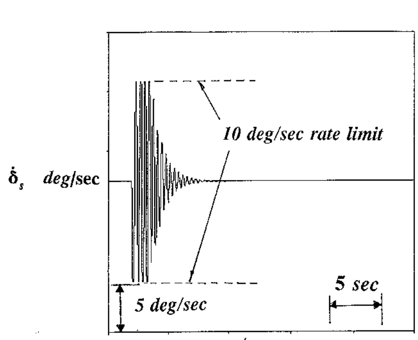

Fig. 21 Stabilator rate after reconfiguration.

Discussion

The relative long adaptation times with a number of the failures in which reconfiguration occurred deserves some comment. The adaptive logic for changing K_D is quite rudimentary, and no attempt was made to improve the speed of convergence for this study. Although the requirement of SCAS stability in the event of failure eliminates the necessity of very rapid reconfiguration, improvement is certainly warranted in this area and is currently being pursued. Note, however, that SCAS performance is improving at each iteration of the adaptive logic. The process could be terminated prematurely by the pilot if he/she so desires. Finally, the longer adaptation times were typically associated with the most severe of the actuator failures in which pilot/vehicle instability resulted when no reconfiguration was undertaken.

The extension of the technique discussed herein to MIMO systems is straightforward in theory. Test inputs would be alternated between control loops in the MIMO application, with the obvious penalty being increased adaptation times. As mentioned earlier one disadvantage of the methodology lies in the high-frequency amplification of pilot inputs created by the reconfigured prefilter $F'(s)$. Reference 23 discusses a MIMO application in which the feedback topology is changed from that of Fig. 3 and in which the adaptation is made much more quickly. The possibility of biodynamic feedback through the control effector is a concern in these cases,[24] as is the possibility that the reconfigured prefilter may increase the deleterious effects of damaged actuators wherein the damage affects the rate limit of the device. Finally, although the reconfiguration scheme allows recapture of much of the performance lost through actuator failure, it is doubtful whether the methodology can provide level one handling qualities for all the failures in the cases that were modeled.

Conclusions

1) A QFT-based loop shaping design technique can offer an approach to reconfigurable control systems when combined with adaptive logic that recovers performance lost in the failure.

2) If a class of failures can be defined, compensators can be designed to maintain stability in the presence of these failures. Identification of system dynamics in the presence of the failures can be avoided.

3) The primary disadvantages of the approach are a) the iterative and time-consuming examination of vehicle response characteristics in the adaptation process and b) the fact that failures outside the bounds of those considered in the class may not be amenable to successful reconfiguration.

Appendix A: Nominal Vehicle Model

Nominal flight condition at altitude of 30,000 ft and Mach number of 0.6

$$\dot{\boldsymbol{x}}(t) = \boldsymbol{A}\boldsymbol{x}(t) + \boldsymbol{B}\boldsymbol{u}(t), \qquad \boldsymbol{x}(t) = [\alpha(t) \quad q(t)]$$

where α is angle of attack, deg; q is pitch rate, deg/s; δ_E is stabilator angle, deg; and δ_{TV} is thrust vector angle, deg and

$$\boldsymbol{A} = \begin{bmatrix} -0.5088 & 0.994 \\ -1.131 & -0.2804 \end{bmatrix}, \qquad \boldsymbol{B} = \begin{bmatrix} -0.9277 & -0.01787 \\ -6.575 & -1.525 \end{bmatrix}$$

The actuator descriptions are, for the stabilator,

$$30^2/(s^2 + 42.4s + 30^2)$$

where the amplitude limit is ±30 deg and the rate limit is 60 deg/s. The thrust vector is

$$20^2/(s^2 + 24s + 20^2)$$

where the amplitude limit is ±30 deg and the rate limit is 60 deg/s.

The cockpit force/feel system dynamics are written

$$25^2/(s^2 + 35s + 25^2)$$

Appendix B: Actuator Failure Models

In the case for the stabilator

$$30^2/(s^2 + 42.4s + 30^2) \cdot K_E e^{-\tau_E s}$$

$$0 \le K_E \le 1.0, \quad 0 \le \tau_E \le 0.4 \text{ s}$$

and for the thrust vector

$$20^2/(s^2 + 24s + 20^2) \cdot K_T e^{-\tau_T s}$$

$$0 \le K_T \le 1.0, \quad 0 \le \tau_T \le 0.4 \text{ s}$$

There are 35 actuator failures created by varying K_E, K_T, τ_E, and τ_T.

Acknowledgment

This work was supported by a Grant from NASA Langley Research Center. The Grant Technical Manager is Barton Bacon.

References

[1]Fulghum, D. A., "Unmanned Strike Next for Military," *Aviation Week and Space Technology*, Vol. 146, No. 23, 1997, pp. 46–48.

[2]Fulghum, D. A., "U.S. Industry Searches for Design Formulas," *Aviation Week and Space Technology*, Vol. 146, No. 23, 1997, pp. 49–50.

[3]Fulghum, D. A., "Payload, not Airframe, Drives UCAV Research," *Aviation Week and Space Technology*, Vol. 146, No. 23, 1997, pp. 51–54.

[4]Fulghum, D. A., "Navy Wants UCAV's for Carrier Use," *Aviation Week and Space Technology*, Vol. 146, No. 23, 1997, p. 55.

[5]"Aviation Safety and Pilot Control," Rept. of the Committee on the Effects of Aircraft-Pilot Coupling on Flight Safety, National Academy Press, Washington, DC, 1997.

[6]Ostroff, A. J., and Hueshcen, R. M., "Investigation of Control Law Reconfiguration to Accommodate a Control Element Failure on a Commercial Aircraft," *Proceedings of the 1984 American Control Conference*, IEEE Service Center, Piscataway, NJ, 1984, pp. 1746–1754.

[7]Horowitz, I., "A Quantitative Inherent Reconfiguration Theory for a Class of Systems," *International Journal of Systems Science*, Vol. 16, No. 11, 1985, pp. 1377–1390.

[8]Eslinger, R. A., and Chandler, P. R., "Self-Repairing Flight Control System Program Overview," *IEEE National Aerospace and Electronics Conference*, IEEE Service Center, Piscataway, NJ, 1988, pp. 504–511.

[9]Ochi, Y., and Kanai, K., "Design of Restructurable Flight Control Systems Using Feedback Linearization," *Journal of Guidance, Control, and Dynamics*, Vol. 14, No. 5, 1991, pp. 903–911.

[10]Ward, D. G., and Barron, R. L., "A Self-Designing Receding Horizon Optimal Flight Controller," *Proceedings of the 1995 American Control Conference*, IEEE Service Center, Piscataway, NJ, 1995, pp. 3490–3494.

[11]Dhayagude, N., and Gao, Z., "Novel Approach to Reconfigurable Control Systems Design," *Journal of Guidance, Control, and Dynamics*, Vol. 19, No. 4, 1996, pp. 963–966.

[12]Kim, B. S., and Calise, A. J., "Nonlinear Flight Control Using Neural Networks," *Journal of Guidance, Control, and Dynamics*, Vol. 20, No. 1, 1997, pp. 26–33.

[13]Keating, M. K., Pachter, M., and Houpis, C. H., "Fault Tolerant Flight Control System: QFT Design," *International Journal of Robust and Nonlinear Control*, Vol. 7, No. 6, 1997, pp. 551–559.

[14]Heiges, M., "Reconfigurable Controls for Rotorcraft," *Journal of the American Helicopter Society*, Vol. 42, No. 3, 1997, pp. 254–263.

[15]Burken, J. J., and Burcham, F. W., Jr., "Flight-Test Results of Propulsion-Only Emergency Control System on MD-11 Airplane," *Journal of Guidance, Control, and Dynamics*, Vol. 20, No. 5, 1997, pp. 980–987.

[16]Hess, R. A., and Snell, S. A., "Flight Control System Design with Rate Saturating Actuators," *Journal of Guidance, Control, and Dynamics*, Vol. 20, No. 1, 1997, pp. 90–96.

[17]Hess, R. A., "Unified Theory for Aircraft Handling Qualities and Adverse Aircraft–Pilot Coupling," *Journal of Guidance, Control, and Dynamics*, Vol. 20, No. 6, 1997, pp. 1141–1148.

[18]Henderson, D. K., and Hess, R. A., "Approximations for Quantitative Feedback Theory Designs," *Journal of Guidance, Control, and Dynamics*, Vol. 20, No. 4, 1997, pp. 828–830.

[19]Adams, R. J., Buffington, J. M., Sparks, A. G., and Banda, S. S., "An Introduction to Multivariable Flight Control System Design," WL-TR-92-3110, Flight Dynamics Directorate, Wright–Patterson AFB, OH, Oct. 1992.

[20]Zeyada, Y., and Hess, R. A., "PVD_{NL} Pilot/Vehicle $\text{Dynamics}_{\text{NonLinear}}$ an Interactive Computer Program for Modeling the Human Pilot in Single-Axis Linear and Nonlinear Tracking Tasks," Dept. of Mechanical and Aeronautical Engineering, Univ. of California, Davis, CA, 1998.

[21]Smith, R. H., "Predicting and Validating Fully Developed PIO" AIAA Paper 94-3669, Aug. 1994.

[22]Osder, S., "Practical View of Redundancy Management Application and Theory," *Journal of Guidance, Control, and Dynamics*, Vol. 22, No. 1, 1999, pp. 12–21.

[23]Hess, R. A., and McLean, C., "Development of a Design Methodology for Reconfigurable Flight Control Systems," AIAA Paper 2000-0890, Jan. 2000.

[24]Gibson, J. C., and Hess, R. A., "Stick and Feel System Design," AGARD-AG-332, March 1997.